**Geomechanics and Engineering**, *Vol. 23, No. 3 (2020) 275-287*
DOI: https://doi.org/10.12989/gae.2020.23.3.275


# Dynamic response of vertically loaded rectangular barrettes in multilayered viscoelastic soil

Geng Cao[1,2], Ming X. Zhu*[1,2], Wei M. Gong[1,2], Xiao Wang[2] and Guo L. Dai[1,2]

[1]*Key of Laboratory for RC and PRC Structure of Education Ministry, Southeast University, Nanjing 211189, China*
[2]*School of Civil Engineering, Southeast University, Nanjing 211189, China*

*(Received June 6, 2020, Revised August 11, 2020, Accepted October 26, 2020)*

**Abstract.** Rectangular barrettes have been increasingly used as foundations for many infrastructure projects, but the vertical vibration of a barrette has been rarely addressed theoretically. This paper presents an analysis method of dynamic response for a rectangular barrette subjected to a time-harmonic vertical force with the aid of a modified Vlasov foundation model in multilayered viscoelastic soil. The barrette-soil system is modeled as a continuum, the vertical continuous displacement model for the barrette and soil is proposed. The governing equations of the barrette-soil system and the boundary conditions are obtained and the vertical shaft resistance of barrette is established by employing Hamilton's principle for the system and thin layer element, respectively. The physical meaning of the governing equations and shaft resistance is interpreted. The iterative solution algorithm flow is proposed to obtain the dynamic response of barrette. Good agreement of the analysis and comparison confirms the correctness of the present solution. A parametric study is further used to demonstrate the effects of cross section aspect ratio of barrettes, depth of soil column, and module ratio of substratum to the upper soil layers on the complex barrette-head stiffness and the resistance stiffness.

**Keywords:** barrette; multilayered viscoelastic soil; continuum; Hamilton's principle; dynamic response

## 1. Introduction

The rectangular barrettes are the large cross section bored piles (drilled-shafts) constructed as the same as a panel of diaphragm wall. A rectangular barrette has the larger specific surface area than circular pile with the equal cross-sectional area, and can bear the larger vertical load through the shaft friction (Lei *et al*. 2005, 2007a), and can improve the ability to bear the larger horizontal load and moment with the appropriate size and arrangement in a certain direction. In the past few decades, rectangular barrettes have been widely used as the foundations for many tall building, viaducts, subway stations and transmission tower structures (Zhang 2003, Lei *et al*. 2005, Ukritchon and Keawsawasvong 2018).

Considering the research of barrette foundations, the earlier studies have been performed to study the capacity and deformation of barrette by the field tests (Fellenius *et al.* 1999, Ng *et al.* 2000, 2003, Zhang 2003). As to the model tests, Lei and Ng (2007b) studied the shaft resistance behavior of barrette in saprolites by static maintained compression loading tests. Wakil and Nazir (2013) probed the effect of the relative density, aspect ratio and loading direction on the barrette lateral resistance in sand. The theorectical methods are available for the analysis of barrettes including the approximate three-dimensional semi-analytical method employing the Mindlin's solution (Lei *et* 2007a), the composed coefficient technique (El Gendy *et al.* 2018, 2019) and the analytical approach with aid of the Winkler model (Hirai 2014). In particular, Basu *et al.* (2008) made a seminal extension of the settlement model of circular piles proposed by Lee and Xiao (1999) and Vallabhan and Mustsfa (1996), and developed a calculation method for rectangular piles settlement by employing the principle of minimum total potential energy. Seo *et al.* (2009) gave the further comparison of settlement property of the circular and rectangular piles. These works exhibit the significance for the studies of loading response of barrettes. However, these studies mentioned above all concern the static analysis of barrette, barrettes inevitably bear dynamic vertical loads from the superstructure, and few studies have been put forward for the vertically dynamic response.

On the other hand, many literatures also have been reported for the dynamic analysis of circular piles. The related methods include the Winkler foundation model-based analytical and numerical methods (Dotson and Veletsos 1986, Nogami and Konagai 1987, Michaelides *et al.* 1998, Wang *et al*. 2010, Kim and Choi 2017), the finite element (FEM) methods (Kuhlemeyer 1979, Liu and Novak, 1994), the boundary element (BEM) methods (Mamoon 1990, Maeso *et al*. 2005), the finite element and boundary element (FEM-BEM) coupling methods (Padron *et al*. 2007, Millanand and Dominguez 2009, Ai and Li 2015), the rigorous analytical or approximate analytical methods (Mylonakis 2001, Anoyatis and Mylonakis 2012, Zheng *et al*. 2015, 2017a, b, Cui *et al*. 2015, 2018a, b) and the variational methods (Das and Sargand 1999, Gupta and Basu 2018). Among them, Winkler spring models are the

*Corresponding author, Associate Professor
E-mail: zhumingxing @seu.edu.cn

**Copyright © 2020 Techno-Press, Ltd.**

ISSN: 2005-307X (Print), 2092-6219 (Online)

simplest, popular and efficient ones computationally. Despite of the advantages in its ability to simulate nonlinearity, the Winkler model-based methods require empirical calibration for accurate spring and dashpot constants and disregard the continuity of soil medium. The FE, BE and FE-BE coupling methods can obtain the true three dimensional dynamic interaction between the soil and piles, however, there exists the obvious limitations that FEM requires the modeling of boundaries at infinity and the convergence is sensitive to the frequency in BEM. The rigorous analytical or approximate analytical methods take into account the influence of damping in solution process, even so, these methods have a complex solving process and the explicit soil layering is neglected in the most analysis.

In terms of the variational methods, Das and Sargand (1999) made the pioneering contribution to present the dynamic response of a single circular pile subjected to horizontal loading at the head on the basis of works of Sun (1994a). This approach is based on the modified Vlasov foundation model, which was proposed by Vallabhan and Das (1988, 1991a, b) for the static analysis of beams on elastic foundations and has the advantage of accounting for the shear interaction between the adjacent springs over the Winkler spring model. With the same method, Gupta and Basu (2018) achieved the study in vertical vibration of a circular pile. However, the aforementioned studies are confined to the pile embedded in a semi-infinite homogeneous soil or the ending-bearing pile in homogeneous soil deposit. Nevertheless, it is not realistic to assume that the soil under the pile bottom has the infinite thickness or features the same properties as the soil around in engineering practice.

This paper aims to cover the cap in the literature and present a numerical approach based on the modified Vlasov foundation model to analyze the dynamic response of rectangular barrette embedded in multilayered soil resting on a rigid bedrock, and when the barrette is subjected to a vertical harmonic load at the top. The finite soil layers under the barrette base are deem as a soil column with the same cross-sectional area of barrette, i.e., fictitious soil pile proposed by Yang and Wang (2010), Wu *et al*. (2016, 2020) and Cai *et al*. (2020). The rational displacement model is proposed for barrette-soil system. The governing equations, the corresponding boundary conditions and the shaft resistance of barrette along depth direction are derived by employing Hamilton's principle and variational calculus. An iterative algorithm procedure is executed to uncouple displacement functions of the barrette, soil column and the soil stratum. Then, the proposed method is verified by comparing special cases of our model with the existing solutions. Finally, some examples are performed to investigate the influence of cross section aspect ratio, depth of soil column and soil layer module ratio on the dynamic response of barrette.

## 2. Statement of the problem

A rectangular barrette with dimensions $B_x \times B_y$, cross-sectional area $A=B_x \times B_y$, length $L$, Young's modulus $E_b$ and density $\rho_b$ is embedded in a total of $n$ viscoelastic soil

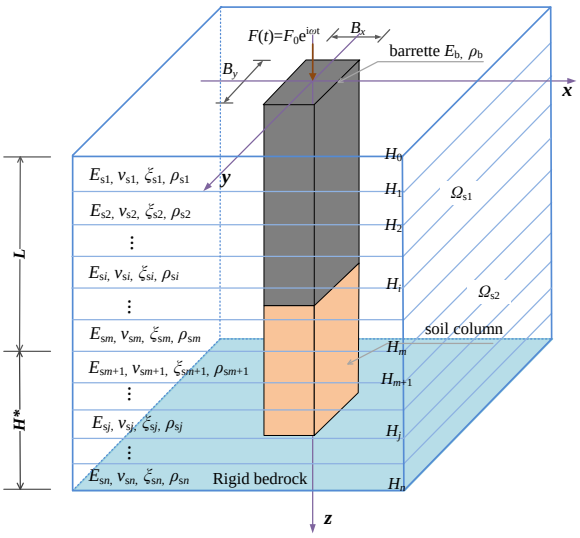


Fig. 1 The vertically loaded rectangular barrette in multilayered viscoelastic soil

stratum resting on the rigid bedrock. The barrette crosses over $m$ soil layers, and there are $n$-$m$ soil layers below the barrette base. $H^*$ is the thickness of the substratum layer, extending from the barrette base to rigid bedrock. The soil underneath the barrette base is assumed to be rectangular soil column with the area of barrette. The barrette head is subjected to an axial steady-state harmonic load with $F(t)=F_0 e^{i\omega t}$ where $\omega$=circular forcing frequency, $F_0$=applied force amplitude, and $t$=time in Fig. 1. The barrette head is flush with the ground surface. The vertical depth of the $i$th intermediate layer's bottom to the ground surface is defined as $H_i$, and the depth of the ground surface is considered as $H_0=0$. The barrette-soil system is modeled as a continuum, and each soil layer is considered as homogeneous, isotropic, and viscoelastic material with a density of $\rho_{si}$, Poisson's ratio of $\nu_{si}$, Young's modulus of $E_{si}$ and hysteretic damping ratio of $\xi_{si}$. Lame's constant of soil $\mu_{si}=E_{si}/\{2(1+\nu_{si})\}$ $\lambda_{si}=E_{si}\nu_{si}/\{(1+\nu_{si})(1-2\nu_{si})\}$, and the complex Lame's constant (Kramer 1996) $\mu_{si}^* = \mu_{si}(1+2i\xi_{si})$ and $\lambda_{si}^* = \lambda_{si}(1+2i\xi_{si})$, where the subscript $i$ denotes the $i$th layer.

The horizontal soil displacements generated by the axially loaded barrette are ignored in this study, the similiar assumption is employed in the vertical settlement analysis of piles (Basu *et al.* 2008, Seo *et al*. 2009, Lee and Xiao 1999, Vallabhan and Mustsfa 1996). The vertical soil displacement field is given as a separation of a displacement function and is mathematically expressed in the following manner

$$g_z(x,y,z,t)=\begin{cases} w(z,t)u(x)v(y), & 0\le z\le L \\ w_s(z,t)u(x)v(y), & L\le z\le H_n \end{cases} \quad (1)$$

where $w(z,t)=w(z)e^{i\omega t}$ represents the vertical barrette displacement (with a dimension of length) along the $z$-direction when $z\le L$, and $w_s(z,t)=w_s(z)e^{i\omega t}$ denotes the vertical displacement of rectangular soil column when $L\le z\le H$. $u(x)$ and $v(y)$ are the dimensionless displacement decay function along the $x$ and $y$ axes, respectively. To ensure proper barrette–soil contact and no slippage or

separation, the values of the functions $u(x)$ and $v(y)$ should be 1 for $-B_x/2 \le x \le B_x/2$ and $-B_y/2 \le y \le B_y/2$, and $u(x) = v(y) = 0$ at $x = \pm\infty$ and $y = \pm\infty$.

## 3. Mathematical formulations of the barrette-soil system and solutions

### 3.1 Governing equation of the barrette-soil system

According to elasticity, the non-zero components of strains can be expressed by the displacements as follows

$$\{\varepsilon_{zz}, \varepsilon_{xz}, \varepsilon_{yz}\}^T = \left\{-\frac{\partial g_z}{\partial z}, -\frac{1}{2}\frac{\partial g_z}{\partial x}, -\frac{1}{2}\frac{\partial g_z}{\partial y}\right\}^T \tag{2}$$

Likewise, the nonzero stress components corresponding to the non-zero components of strains can be given as

$$\{\sigma_{zz}, \tau_{xz}, \tau_{yz}\}^T = \left\{-\left(\lambda_s^* + 2\mu_s^*\right)\frac{\partial g_z}{\partial z}, -\mu_s^*\frac{\partial g_z}{\partial x}, -\mu_s^*\frac{\partial g_z}{\partial y}\right\}^T \tag{3}$$

The barrette can be modelled as an elastic axial compression member, and the functional of the potential energy $V$ of barrette-soil system we can give

$$\begin{aligned} V = {} & \int_0^L \frac{1}{2}E_b A\left(\frac{\partial w}{\partial z}\right)^2 dz + \int_L^H \frac{1}{2}E_s A\left(\frac{\partial w_s}{\partial z}\right)^2 dz \\ & + \iiint_{\Omega_{s1}} \frac{1}{2}\left[\left(\lambda_s^* + 2\mu_s^*\right)\left(\frac{\partial w}{\partial z}\right)^2 u^2 v^2 + \mu_s^* w^2\left(\frac{du}{dx}\right)^2 v^2\right. \\ & \left. + \mu_s^* w^2 u^2\left(\frac{dv}{dy}\right)^2\right] dxdydz \\ & + \iiint_{\Omega_{s2}} \frac{1}{2}\left[\left(\lambda_s^* + 2\mu_s^*\right)\left(\frac{\partial w_s}{\partial z}\right)^2 u^2 v^2 + \mu_s^* w_s^2\left(\frac{du}{dx}\right)^2 v^2\right. \\ & \left. + \mu_s^* w_s^2 u^2\left(\frac{dv}{dy}\right)^2\right] dxdydz \end{aligned} \tag{4}$$

where the $\Omega_{s1}$ and $\Omega_{s2}$ denote the infinitesimally horizontal soil domain outside the barrette and soil column, respectively. The first and second items represent the energy from the compression of barrette and soil column, and the third and fourth items account for the strain energy of the soil domain surrounding the barrette and soil column.

The kinetic energy $T$ of the barrette-soil system is shown to be

$$\begin{aligned} T = {} & \int_0^L \frac{1}{2}\rho_b A\left(\frac{\partial w}{\partial t}\right)^2 dz + \int_L^H \frac{1}{2}\rho_s A\left(\frac{\partial w_s}{\partial t}\right)^2 dz \\ & + \iiint_{\Omega_{s1}} \frac{1}{2}\rho_s\left[\frac{\partial(wuv)}{\partial t}\right]^2 dxdydz \\ & + \iiint_{\Omega_{s2}} \frac{1}{2}\rho_s\left[\frac{\partial(w_s uv)}{\partial t}\right]^2 dxdydz \end{aligned} \tag{5}$$

The kinetic energy $T$ is comprised of four items, i.e., the barrette, soil column motion and the soil motion outside the barrette and the soil column.

For the work $W$ performed by the vertical force $F(t)$, we have

$$W = F\,w\big|_{z=0} \tag{6}$$

The vibrations of the system are governed by Hamilton's variational principle (Dym *et al*. 1973)

$$\int_{t_1}^{t_2} \delta(T - V)dt + \int_{t_1}^{t_2} \delta W dt = 0 \tag{7}$$

where $\delta(\cdot)$ denotes a variation. The variable $t$ is of course the time.

Performing the partial integration on the terms associated with $\delta(\partial w/\partial t)$ and $\delta\{\partial(wuv)/\partial t\}$ with respect to $t$, similarly, $\delta(\partial w_s/\partial t)$ and $\delta\{\partial(w_s uv)/\partial t\}$ with respect to $t$, $\delta(\partial w/\partial z)$ with respect to $z$, and $\delta(\partial u/\partial x)$ and $\delta(\partial v/\partial y)$ with respect to $x$ and $y$, respectively in Eq. (7). The governing equation of the barrette-soil system can be obtained.

### 3.2 Displacement of the barrette and soil column

Collecting the items with $\delta w$ and $\delta w_s$ and considering the multilayered soil stratum, we get the following equation

$$\begin{aligned} & \sum_{i=1}^{m}\int_{H_{i-1}}^{H_i}\left(E_b A\frac{\partial^2 w_i}{\partial z^2} - k_i w_i + t_i\frac{\partial^2 w_i}{\partial z^2} - \kappa\rho_{si}\frac{\partial^2 w_i}{\partial t^2} - \rho_b A\frac{\partial^2 w_i}{\partial t^2}\right)\delta w_i dz \\ & + \sum_{i=m+1}^{n}\int_{H_{i-1}}^{H_i}\left(E_{si}A\frac{d^2 w_{si}}{dz^2} - k_i w_{si} + t_i\frac{\partial^2 w_{si}}{\partial z^2} - \kappa\rho_{si}\frac{\partial^2 w_{si}}{\partial t^2} - \rho_{si}A\frac{\partial^2 w_{si}}{\partial t^2}\right. \\ & \left. - \rho_{si}A\frac{\partial^2 w_{si}}{\partial t^2}\right)\delta w_{si} dz + \sum_{i=1}^{m}\left[-E_b A\frac{\partial w_i}{\partial z}\delta w_i\Big|_{H_{i-1}}^{H_i} - t_i\frac{\partial w_i}{\partial z}\delta w_i\Big|_{H_{i-1}}^{H_i}\right] \\ & + \sum_{i=m+1}^{n}\left[-E_{si}A\frac{\partial w_{si}}{\partial z}\delta w_{si}\Big|_{H_{i-1}}^{H_i} - t_i\frac{\partial w_{si}}{\partial z}\delta w_{si}\Big|_{H_{i-1}}^{H_i}\right] + F\,\delta w\big|_{z=0} = 0 \end{aligned} \tag{8}$$

where

$$k_i = \iint_{Dxy}\mu_{si}^*\left(\frac{du}{dx}\right)^2 v^2 dxdy + \iint_{Dxy}\mu_{si}^*\left(\frac{dv}{dy}\right)^2 u^2 dxdy \tag{9}$$

$$t_i = \iint_{Dxy}\left(\lambda_{si}^* + 2\mu_{si}^*\right)u^2 v^2 dxdy \tag{10}$$

$$\kappa = \iint_{Dxy} u^2 v^2 dxdy \tag{11}$$

Since the variation of $w_i$ is unknown previously within $H_{i-1} < z < H_i$, $(i = 1,2,\ldots,m)$, $\delta w_i \neq 0$, the governing equation of barrette can be obtained

$$E_b A\frac{\partial^2 w_i}{\partial z^2} - k_i w_i + t_i\frac{\partial^2 w_i}{\partial z^2} - \kappa\rho_{si}\frac{\partial^2 w_i}{\partial t^2} - \rho_b A\frac{\partial^2 w_i}{\partial t^2} = 0 \tag{12}$$

The five terms with different physical mechanisms are included in the dynamic equilibrium equation (12). The first term represents the axial resistances as the compression of the barrette; the second term describes the resistance of soil against shearing and can be considered as Winkler spring constant; the third term quantifies the soil resistance generated from the soil compression; the fourth indicates the vertical inertia forces of soil around the barrette; the fifth item represents the axial inertia forces of the barrette. The sum of the second, the third and the fourth represents the dynamic shaft resistance of barrette and the physical mechanisms will be interpreted later on.

Similarly, $\delta w_{si} \neq 0$ since the variation of $w_{si}$ is not known

within $H_{i-1}<z<H_i$, ($i=m+1,\ldots,n-1$) we get the governing equation of soil column

$$E_s A\frac{\partial^2 w_{si}}{\partial z^2}-k_i w_{si}+t_i\frac{\partial^2 w_{si}}{\partial z^2}-\kappa\rho_{si}\frac{\partial^2 w_{si}}{\partial t^2}-\rho_s A\frac{\partial^2 w_{si}}{\partial t^2}=0 \quad (13)$$

Furthermore, substitution of $w(z,t)=w(z)e^{i\omega t}$ in Eq. (12) gives

$$\left(E_b A+t_i\right)\frac{d^2 w_i}{dz^2}-\left\{k_i-\left(\rho_p A+\kappa\rho_{si}\right)\omega\right\}w_i=0 \quad (14)$$

Substitution of $w_s(z,t)=w_s(z)e^{i\omega t}$ in Eq. (13) gives

$$\left(E_{si}A+t_i\right)\frac{d^2 w_{si}}{dz^2}-\left\{k_i-\left(\rho_{si}A+\kappa\rho_{si}\right)\omega^2\right\}w_{si}=0 \quad (15)$$

The boundary condition at the (i.e., $z=0$) is given by

$$\left(E_b A+t_1\right)\left.\frac{dw_1}{dz}\right|_{z=0}=-F_0 \quad (16)$$

The Eq. (16) means that the vertically applied load is equal to the axial force at the barrette head.

At the interface between the $i$th and ($i$+1)th soil layer ($i=1,2,\ldots,m-1$), the boundary conditions are given by

$$\left.w_i\right|_{z=H_i}=\left.w_{i+1}\right|_{z=H_i} \quad (17)$$

$$\left(E_b A+t_i\right)\left.\frac{dw_i}{dz}\right|_{z=H_i}=\left(E_b A+t_{i+1}\right)\left.\frac{dw_{i+1}}{dz}\right|_{z=H_i} \quad (18)$$

At the barrette base ($z=L$), the boundary conditions are

$$\left.w_m\right|_{z=L}=\left.w_{s,m+1}\right|_{z=L} \quad (19)$$

$$\left(E_b A+t_m\right)\left.\frac{dw_m}{dz}\right|_{z=L}=\left(E_{s,m+1}A+t_{m+1}\right)\left.\frac{dw_{s,m+1}}{dz}\right|_{z=L} \quad (20)$$

Similarly, at the interface between the $i$th and ($i$+1)th layer ($i=m+1,\ldots,n-1$) within soil column the boundary conditions are derived as

$$\left.w_{s,i}\right|_{z=H_i}=\left.w_{s,i+1}\right|_{z=H_i} \quad (21)$$

$$\left(E_{si}A+t_i\right)\left.\frac{dw_{si}}{dz}\right|_{z=H_i}=\left(E_{s,i+1}A+t_{i+1}\right)\left.\frac{dw_{s,i+1}}{dz}\right|_{z=H_i} \quad (22)$$

At the soil column base ($z=H_n$), the boundary conditions is

$$\left.w_s\right|_{z=H_n}=0 \quad (23)$$

The general solutions of Eqs. (14) and (15) are given by

$$w_i(z)=c_{1i}e^{r_{bi}z}+c_{2i}e^{-r_{bi}z}\quad i=1,2,\ldots,m \quad (24a)$$

$$w_{si}(z)=c_{1i}e^{r_{si}z}+c_{2i}e^{-r_{si}z}\quad i=m+1,\ m+2,\ldots,n \quad (24b)$$

where $c_{1i}$ and $c_{2i}$ are unknown constants for the $i$th layer. The parameters $r_{bi}$ and $r_{si}$ are given by

$$r_{bi}=\sqrt{\frac{k_i-\left(\rho_p A+\kappa\rho_{si}\right)\omega^2}{E_b A+t_i}}\quad i=1,2,\ldots,m \quad (25a)$$

$$r_{si}=\sqrt{\frac{k_i-\left(\rho_{si}A+\kappa\rho_{si}\right)\omega^2}{E_{si}A+t_i}}\quad i=m+1,\ m+2,\ldots,n \quad (25b)$$

In Eqs. (24a) and (24b) there are $2n$ unknown constants for a total of $n$ layer soil stratum. Eqs. (17)-(22) produce $2n$-2 boundary condition equations at the. $n$-1 interfaces (two equations at each interface), and Eqs. (16) and (23) produce 2 boundary-condition equations at the barrette head and the soil column base, respectively. This results in a matrix equation consisting of the $2n$ unknown constants and we express the equations in matrix form in Appendix A.

### 3.3 Decay functions u and v for soil displacement

Collecting the coefficients of $\delta u$, we then get the governing equation for the decay function $u(x)$

$$\frac{d^2 u}{dx^2}-\alpha^2 u=0 \quad (26)$$

where

$$\alpha=\sqrt{\alpha_2/\alpha_1} \quad (27)$$

$$\alpha_1=\int v^2 dy\left(\sum_{i=1}^{m}\int_{H_{i-1}}^{H_i}\mu_{si}^* w_i^2 dz+\sum_{i=m+1}^{n}\int_{H_{i-1}}^{H_i}\mu_{si}^* w_{si}^2 dz\right) \quad (28)$$

$$\begin{aligned}\alpha_2=&-\omega^2\int v^2 dy\left(\sum_{i=1}^{m}\int_{H_{i-1}}^{H_i}\rho_{si}w_i^2 dz+\sum_{i=m+1}^{n}\int_{H_{i-1}}^{H_i}\rho_{si}w_{si}^2 dz\right)\\&+\int v^2 dy\left[\sum_{i=1}^{m}\int_{H_{i-1}}^{H_i}\left(\lambda_{si}^*+2\mu_{si}^*\right)\left(\frac{dw_i}{dz}\right)^2 dz\right.\\&\left.+\sum_{i=m+1}^{n}\int_{H_{i-1}}^{H_i}\left(\lambda_{si}^*+2\mu_{si}^*\right)\left(\frac{dw_{si}}{dz}\right)^2 dz\right]\\&+\int\left(\frac{dv}{dy}\right)^2 dy\left(\sum_{i=1}^{m}\int_{H_{i-1}}^{H_i}\mu_{si}^* w_i^2 dz+\sum_{i=m+1}^{n}\int_{H_{i-1}}^{H_i}\mu_{si}^* w_{si}^2 dz\right)\end{aligned} \quad (29)$$

with the boundary conditions $x=\pm B_x/2$, $u=1$and $x=\pm\infty$, $u=0$.

For the boundary conditions $u$, the solution of $u(x)$ is given by

$$u(x)=\begin{cases}e^{\alpha(x+B_x/2)}, -\infty<x\le -B_x/2\\ e^{-\alpha(x-B_x/2)}, B_x/2\le x<+\infty\end{cases} \quad (30)$$

Similarly, collecting the coefficients of $\delta v$, we have the governing equation for the function $v(x)$ as follows:

$$\frac{d^2 v}{dy^2}-\beta^2 v=0 \quad (31)$$

along with the boundary conditions $y=\pm B_y/2$, $v=1$ and $y=\pm\infty$, $v=0$.

Where

$$\beta=\sqrt{\beta_2/\beta_1} \quad (32)$$

$$\beta_1=\int u^2 dx\left(\sum_{i=1}^{m}\int_{H_{i-1}}^{H_i}\mu_{si}^* w_i^2 dz+\sum_{i=m+1}^{n}\int_{H_{i-1}}^{H_i}\mu_{si}^* w_{si}^2 dz\right) \quad (33)$$

$$\begin{aligned}&\iint_{Dxy}\rho_{si}\frac{\partial(w_i uv)}{\partial t}dxdydz\delta(w_i uv)\Big|_{t_1}^{t_2}-\int_{t_1}^{t_2}\iint_{Dxy}\rho_{si}\frac{\partial^2 w_i}{\partial^2 t}uv\delta(w_i uv)dxdydzdt\\&-\int_{t_1}^{t_2}\left\{\iint_{Dxy}\left[\left(\lambda_{si}^*+2\mu_{si}^*\right)\frac{\partial w_i}{\partial z}\delta\left(\frac{\partial w_i}{\partial z}\right)u^2v^2+\left(\lambda_{si}^*+2\mu_{si}^*\right)\left(\frac{\partial w_i}{\partial z}\right)^2u\delta uv^2+\left(\lambda_{si}^*+2\mu_{si}^*\right)\left(\frac{\partial w_i}{\partial z}\right)^2u^2v\delta v+\mu_{si}^*w_i\delta w_i\left(\frac{du}{dx}\right)^2v^2\right.\right.\\&\left.\left.+\mu_{si}^*w_i^2\frac{du}{dx}\delta\left(\frac{du}{dx}\right)v^2+\mu_{si}^*w_i^2\left(\frac{du}{dx}\right)^2v\delta v+\mu_{si}^*w_i\delta w_iu^2\left(\frac{dv}{dy}\right)^2+\mu_{si}^*w_i^2u\delta u\left(\frac{dv}{dy}\right)^2+\mu_{si}^*w_i^2u^2\frac{dv}{dy}\delta\left(\frac{dv}{dy}\right)\right]dxdydzdt\right.\\&\left.+\int_{t_1}^{t_2}\left[\iint_{Dxy}\left(\lambda_{si}^*+2\mu_{si}^*\right)\delta\left(\frac{\partial^2 w_i}{\partial z^2}w_iu^2v^2\right)dxdydz+\tau_i(z,t)\delta w_i dz\right]dt=0\end{aligned}\tag{40}$$

$$\begin{aligned}\beta_2=&-\omega^2\int u^2dx\left(\sum_{i=1}^{m}\int_{H_{i-1}}^{H_i}\rho_{si}w_i^2dz+\sum_{i=m+1}^{n}\int_{H_{i-1}}^{H_i}\rho_{si}w_{si}^2dz\right)\\&+\int u^2dx\left[\sum_{i=1}^{m}\int_{H_{i-1}}^{H_i}\left(\lambda_{si}^*+2\mu_{si}^*\right)\left(\frac{dw_i}{dz}\right)^2dz\right.\\&\left.+\sum_{i=m+1}^{n}\int_{H_{i-1}}^{H_i}\left(\lambda_{si}^*+2\mu_{si}^*\right)\left(\frac{dw_{si}}{dz}\right)^2dz\right]\\&+\int\left(\frac{du}{dx}\right)^2dx\left(\sum_{i=1}^{m}\int_{H_{i-1}}^{H_i}\mu_{si}^*w_i^2dz+\sum_{i=m+1}^{n}\int_{H_{i-1}}^{H_i}\mu_{si}^*w_{si}^2dz\right)\end{aligned}\tag{34}$$

For the boundary conditions $v$, the solution of $v(y)$ is given by

$$v(y)=\begin{cases}e^{\beta(y+B_y/2)}, -\infty<y\le -B_y/2\\ e^{-\beta(y-B_y/2)}, B_y/2\le y<+\infty\end{cases}\tag{35}$$

### 3.4 Solution algorithm

It can be observed that the displacement functions $w(z)$ and $w_s(z)$ is coupled with the function $u(x)$ and $v(y)$, herein, an iterative algorithm similar to Vallabhan and Das (Vallabhan *et al*. 1988, 1991a, b) is executed to obtain the solutions in this study. The basic steps are as follows.

(1) The initial values of parameters $\alpha$ and $\beta$ are guessed, for example $\alpha$=$\beta$=1.

(2) The functions $u(x)$ and $v(y)$ are determined from Eq. (30) and (35).

(3) Calculate the values of $t_i$, $k_i$ and $\kappa$ in Eqs. (9)-(11).

(4) Calculate the values of $r_{bi}$ and $r_{si}$ in Eqs. (25a) and (25b).

(5) Assemble the matrix Eq. (A-1), and solve the barrette and soil column displacements $w_i(z)$ and $w_{si}(z)$ by Eqs. (24a) and (24b).

(6) A new values of $\alpha$ and $\beta$ are obtained by Eqs. (27), (28) and (29) and Eqs. (32), (33) and (34), respectively.

(7) Check if the difference of new $\alpha$ and $\beta$ with the olds.

(8) Repeat steps (1)-(7) until the absolute difference between new $\alpha$ and $\beta$ and the olds fall below a prescribed tolerable limit, such as 1/1000.

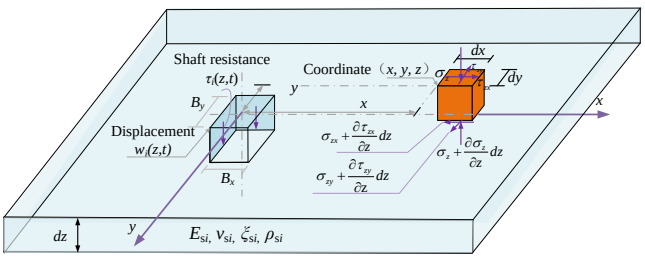


Fig. 2 The external force on the thin layer element

## 4. Physical mechanisms of the proposed model

The thin layer element of the soil is intercepted at the depth $z$ within the $i$th soil layer ($H_{i-1}$<$z$<$H_i$, $i$=1,2,…,$m$), as indicates in Fig. 2. The potential energy $V_{\text{layer}}$ of thin layer element with the thickness $dz$ is given by the form of strain and stress components

$$V_{\text{layer}}=\frac{1}{2}\iint_{Dxy}[\sigma_{zz}\varepsilon_{zz}+2(\tau_{xz}\varepsilon_{xz}+\tau_{yz}\varepsilon_{yz})]dxdydz\tag{36}$$

The kinetic energy $T_{\text{layer}}$ of the thin layer element is

$$T_{\text{layer}}=\iint_{Dxy}\frac{1}{2}\rho_{si}\left(\frac{\partial g_z}{\partial t}\right)^2dxdydz\tag{37}$$

The work $W_{\text{layer}}$ of the thin layer element performed by the external force is given

$$W_{\text{layer}}=\iint_{Dxy}\frac{\partial\sigma_z}{\partial z}g_z dxdydz+\tau_i(z,t)w_i dz\tag{38}$$

Hamilton's variational principle is employed for the thin layer element as follows

$$\begin{aligned}&\int_{t_1}^{t_2}\delta\left\{\iint_{Dxy}\frac{1}{2}\rho_{si}\left(\frac{\partial g_z}{\partial t}\right)^2dxdydz\right.\\&\left.-\frac{1}{2}\iint_{Dxy}[\sigma_{zz}\varepsilon_{zz}+2(\tau_{xz}\varepsilon_{xz}+\tau_{yz}\varepsilon_{yz})]dxdydz\right\}dt\\&+\int_{t_1}^{t_2}\delta\left[\iint_{Dxy}\frac{\partial\sigma_z}{\partial z}g_z dxdydz+\tau_i(z,t)w_i dz\right]dt=0\end{aligned}\tag{39}$$

Performing the partial integration on the terms associated with $\delta\{\partial(w_i uv)/\partial t\}$ with respect to $t$, we get Eq. (40). Collecting all the terms associated with $\delta w_i$ in Eq. (40) and equating their sum to zero, the following equation can be got

$$\begin{aligned}&\int_{t_1}^{t_2}\left\{-\iint_{Dxy}\rho_{si}u^2v^2dxdy\frac{\partial^2 w_i}{\partial^2 t}\right.\\&-\iint_{Dxy}\left[\mu_{si}^*\left(\frac{du}{dx}\right)^2v^2+\mu_{si}^*u^2\left(\frac{dv}{dy}\right)^2\right]w_i dxdy\\&\left.+\iint_{Dxy}\left(\lambda_{si}^*+2\mu_{si}^*\right)u^2v^2\frac{\partial^2 w_i}{\partial z^2}dxdy+\tau_i(z,t)\right\}\delta w_i dzdt=0\end{aligned}\tag{41}$$

We obtain the dynamic shaft resistance $\tau_i(z,t)$ of axially loaded barrette as follows

$$\tau_i(z,t)=k_i w_i-t_i\frac{\partial^2 w_i}{\partial z^2}+\kappa\rho_{si}\frac{\partial^2 w_i}{\partial t^2}\tag{42}$$

The dynamic shaft resistance of barrette is composed of three individual parts: the first part is the linear term of the displacement $w_i$ and is considered as the so-called Winkler

spring $k_i$, and we can find from the deduction of Eqs. (39), (40) and (41) that Winkler spring $k_i$ is produced by the shearing stress $\tau_{xz}$ and $\tau_{yz}$ in soil layer. The second part is generated from the stress $\sigma_z$ as a result of the modified Vlasov foundation model, and this part accounts for the interaction of Winkler spring $k_i$. The third part denotes to the contribution of the participating mass of the soil surrounding the barrette.

The sum of the second, the third and the fourth item in the governing equation (12) is identical to the shaft resistance $\tau_i(z,t)$. Therefore, the governing differential equation of barrette motion is essentially the dynamic equilibrium consisted of axial force, shaft resistance and the vertical inertia force.

The stiffness of the shaft resistance, generally used in elastodynamics, can be obtained by dividing the dynamic shaft resistance by the corresponding settlement.

Substituting the $w_i(z,t)=w_i(z)e^{i\omega t}$ and Eq. (24a) into the Eq. (42), we get the resistance stiffness $p_i$ wihtin the $i$th soil layer as follows

$$p_i = k_i - t_i\left(r_{bi}\right)^2 - \kappa\rho_{si}\omega^2 \tag{43}$$

## 5. Result and discussion

The response for laterally and vertically loaded circulars piles has been creatively studied in the literature (Sun 1994a, 1994b, Vallabhan and Mustsfa 1996 and Lee and Xiao 1999) based on the modified Vlasov foundation model by assuming the rational displacement field in the soil mass. Guo and Lee (2001) and Basu *et al*. (2008) found that the displacement model of the soil-pile system in the Sun's (1994a, 1994b) analysis resulted in artificially stiff pile response. The stiffer load-settlement response of piles than finite element solution are also observed in the analysis ( Vallabhan and Mustsfa 1996 and Lee and Xiao 1999 ). In fact, the soil Lame's constant $\lambda_{si}=E_{si}\nu_{si}/\{(1+\nu_{si})(1-2\nu_{si})\}$ is high sensitive to Poisson's ratio $\nu_{si}$, and when the soil Poisson's ratio $\nu_{si}$ is close to 0.5, $\lambda_{si}$ will be infinity, which causes the incredible stiffer response of pile. In order to remove the artificial stiffness and make the pile response tend to the reality, the modified shear modules (a similar modification was put forward by Randolph 1981) were used in the literatures (Basu *et al*. 2008, Basu and Salgado 2008, Seo *et al*. 2009, Gupta and Basu 2016a, b, Tehrani *et al*. 2016, Gupta and Basu 2017, 2018). So, the Lame's constants $\lambda_{si}$ and $\mu_{si}$ are also replaced in this study by the modified ones $\bar{\lambda}_{si}=0$ and $\bar{\mu}_{si}=0.6\mu_{si}\left(1+1.25\upsilon_{si}^2\right)$, by using which the accuracy of settlement response of rectangular piles was verified against comparing equivalent three-dimensional finite element analysis (Basu *et al*. 2008 and Seo *et al*. 2009).

To facilitate the parametric study, a dimensionless dynamic barrette-head stiffness $K_v$ defined as

$$K_v = \frac{F_0}{\mu_{s1} r_e w_0} \tag{44}$$

where $F_0$= forcing amplitude at the barrette head; $w_0$=settlement at the head; $\mu_{s1}$= shear module in the first soil layer; $r_e$ = equivalent radius ($\sqrt{B_x B_y/\pi}$).

A dimensionless frequency $\alpha_0$ is introduced as

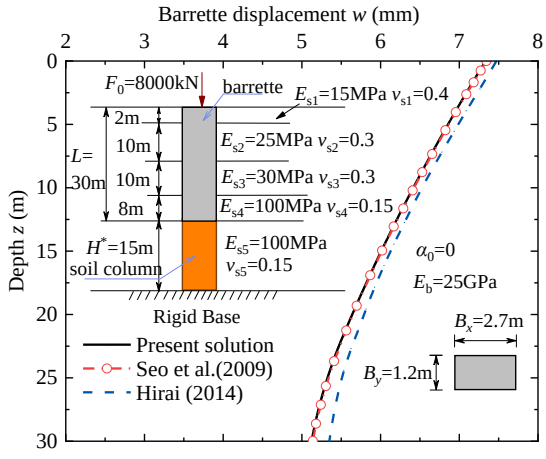


Fig. 3 Comparisons of barrette displacement under dimensionless frequency $\alpha_0$=0 by proposed model with those by Seo *et al*. (2009) and Hirai (2014)

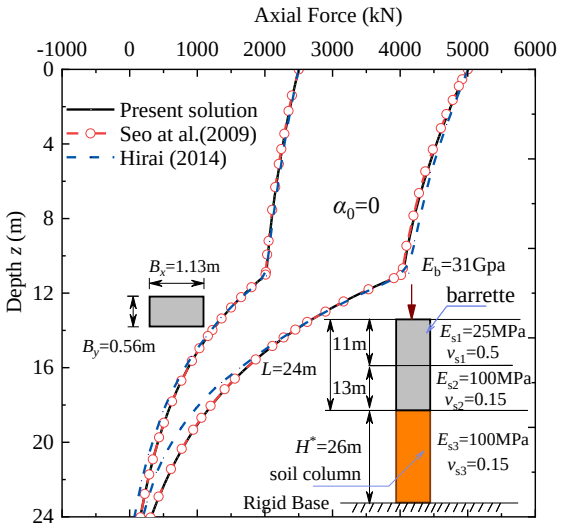


Fig. 4 Comparisons of axial force of barrette under dimensionless frequency $\alpha_0$=0 by proposed model with those by Seo *et al*. (2009) and Hirai (2014)

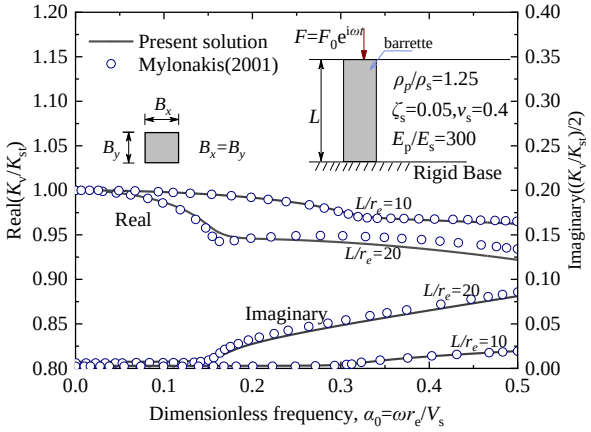


Fig. 5 Comparison of the normalized head stiffness by proposed solution with Mylonakis's solution (2001)

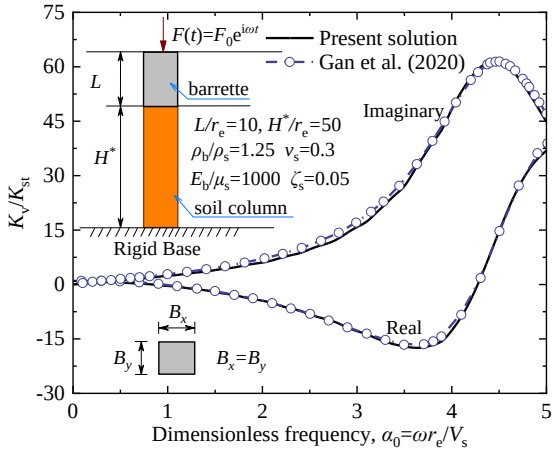


Fig. 6 Comparison of the normalized stiffness by proposed solution with those by Gan *et al*. (2020)

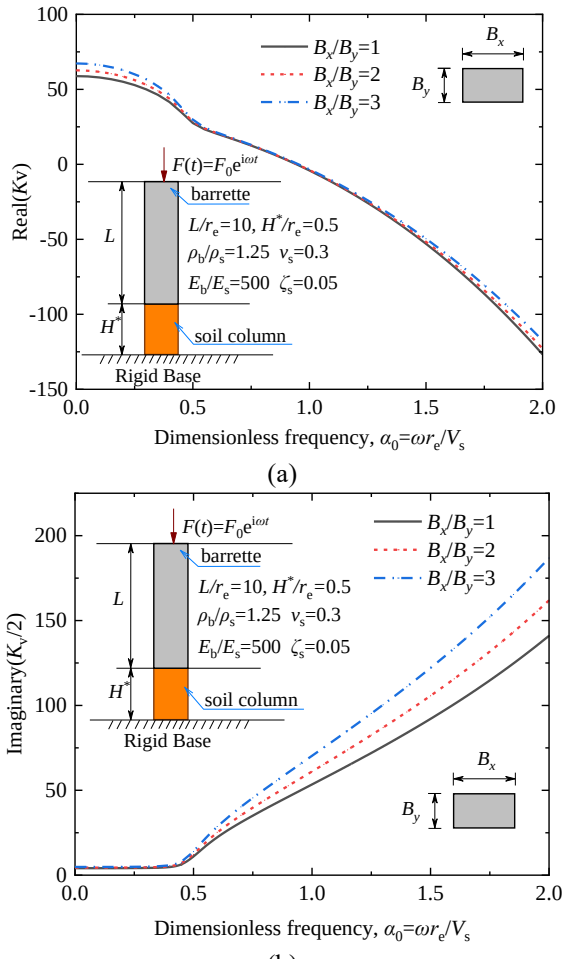


Fig. 7 Effect of aspect ratio of barrette on the complex barrette-head stiffness ($L/r_e$=10)

$$a_0 = \frac{\omega r_e}{V_s} \tag{45}$$

$\omega$= circular forcing frequency; $V_s$= shear wave velocity of the first soil layer ($\sqrt{\mu_{s1}/\rho_{s1}}$). The static barrette-head stiffness is denoted as $K_{st}$ when the circular forcing

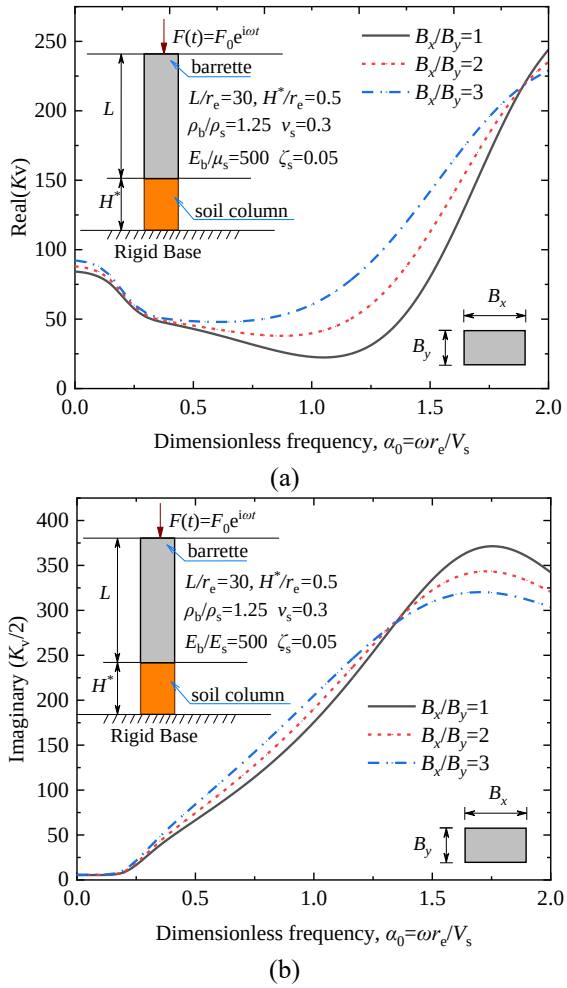


Fig. 8 Effect of aspect ratio of barrette on the complex barrette-head stiffness ($L/r_e$=30)

frequency $\omega$ is equal to zero (i.e., the dimensionless frequency $a_0$=0).

### *5.1 Comparison and verification*

To the author's knowledge, there is no study conducted to solve the dynamic response of rectangular barrettes or piles subjected to a vertical harmonic load. To demonstrate the accuracy of the proposed method, the solutions in this study are firstly degenerated to investigate the response of the vertically loaded barrette with dimensionless frequency $a_0$=0, i.e., under static loading. Fig. 3 and Fig. 4 show the comparison of the vertical displacement and axial force profiles of the barrettes with those by Seo *et al*. (2009) and Hirai (2014). The input parameters used are given in Fig. 3 and Fig. 4, respectively. The results from present method are well agreement with solutions by Seo *et al*. (2009). The reason of good consistence is that the Seo's solutions are the special cases of our present study when the circular forcing frequency $\omega$ is equal to zero. Also, the slight difference between our analysis and Hirai's solution can be observed in that the two methods are used in solution approaches. The modified Vlasov foundation model based on continuum analysis is employed for the barrette responses while the corresponding results from Hirai's

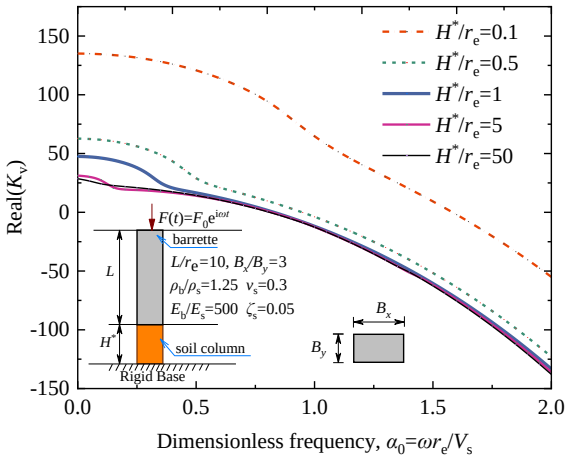


(a)

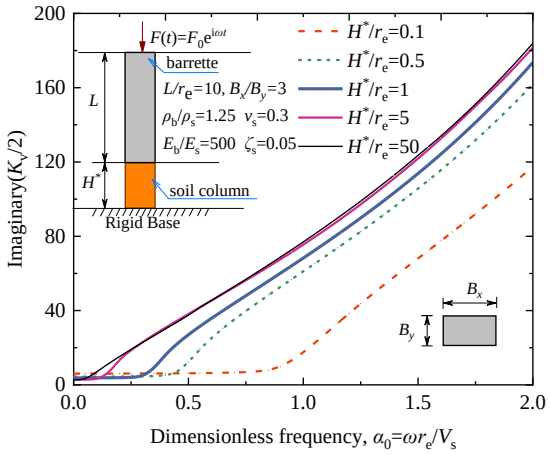


(b)

Fig. 9 Effect of soil column depth on the complex barrette-head stiffness ($L/r_e$=10)

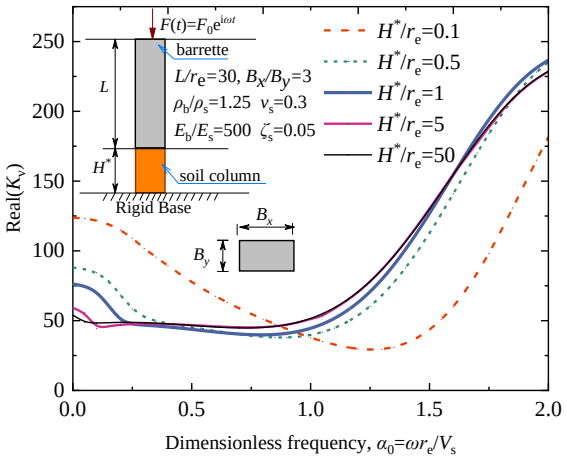


(a)

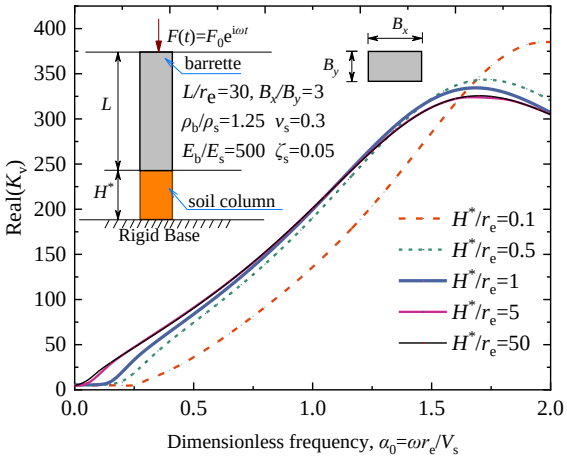


(b)

Fig. 10 Effect of soil column depth on the complex barrette-head stiffness ($L/r_e$=30)

method were performed using a Winkler model approach.

As shown in Fig. 5, a comparison of the normalized square barrette head stiffness $K_v/K_{st}$ from the present model is performed with the results of end-bearing circular piles obtained by Mylonakis (2001), who proposed an approximate continuum-based analytical solution. The square barrette and circular pile maintain the equal cross-sectional area and length, i.e the same equivalent radius and slenderness ratio. The material and geometrical parameters are used as follows: $\rho_b/\rho_s$=1.25, $v_s$=0.4, $\xi_s$=0.05, $E_b/E_s$=300, $B_x$=$B_y$, $0\le a_0\le 1$, $L/r_e$=10 and $L/r_e$=20. As can be seen from the Fig. 5, the normalized head stiffness of square barrette provided by present method are good agreement with the solutions of circular pile given by Mylonakis (2001).

In order to further examine the present method, as shown in Fig. 6, the normalized stiffness of a floating square barrette in viscoelastic soil layer overlaying a rigid base is compared against the analytical solution of floating circular piles proposed by Gan *et al*. (2020) with the equal cross-sectional area and length. The parameters are employed as follows: $\rho_b/\rho_s$=1.25, $v_s$=0.3, $\xi_s$=0.05, $E_b/\mu_s$=1000, $B_x$=$B_y$, $0\le a_0\le 5$, $L/r_e$=10 and $H^*/r_e$=50. Excellent match between the present results and the available solutions (Gan *et al*. 2020) is observed within the range of loading frequency in Fig. 6.

As discussed above, the all agreements confirm the correctness of the proposed model.

### *5.2 Influence of cross sections aspect ratio of rectangular barrette*

Figs. 7 and 8 show the effects of the cross section aspect ratio of rectangular barrettes on the dimensionless dynamic barrette-head stiffness $K_v$ with slenderness ratio $L/r_e$=10 and $L/r_e$=30 for the same substratum layer thickness $H^*/r_e$ =0.5. It is clear that both of the real and imaginary part of barrette-head stiffness increase with the increasing aspect ratio $B_x/B_y$, in that the greater shaft resistance with the increase of the aspect ratio is produced by the larger perimeter of rectangular barrette for the equal cross-sectional area (Seo *et al.* 2009, Hirai 2014). However, the effect of aspect ratio is dependent on the slenderness ratio. The additional stiffness increases slightly with increase in the cross sections aspect ratio for the stubby barrette with slenderness ratio $L/r_e$=10, as shown in Fig. 7, while the increment is more pronounced for the slender pile with $L/r_e$=30 in the frequency range $0.5\le a_0\le 1.75$, as depicted in Fig. 8. Besides, observe by the comparison with Fig. 7 and

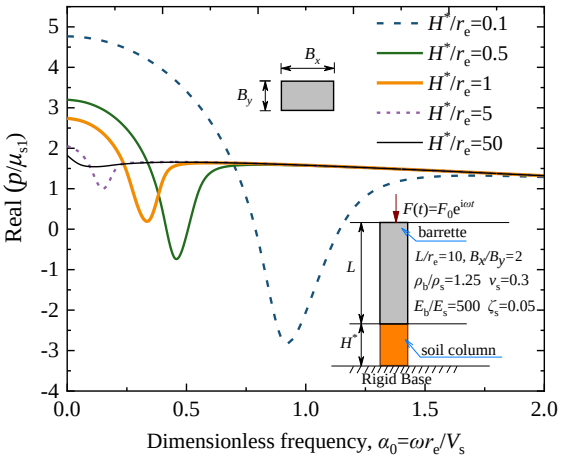


(a)

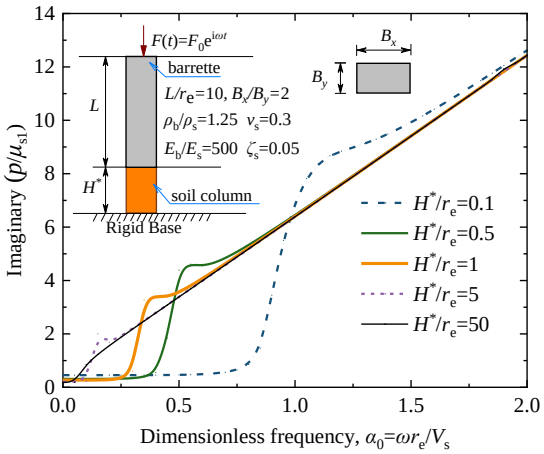


(b)

Fig. 11 Effect of soil column depth on the complex resistance stiffness ($L/r_e$=10)

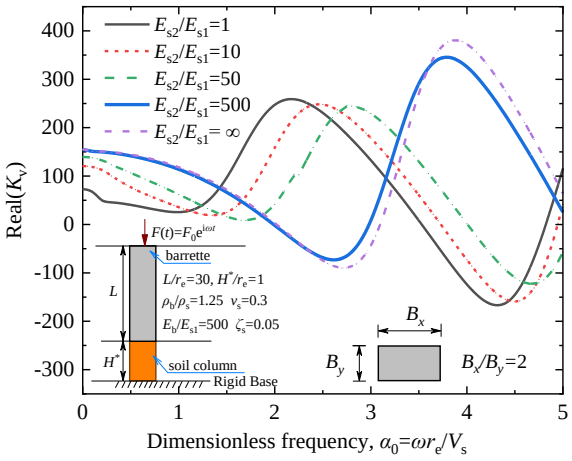


(a)

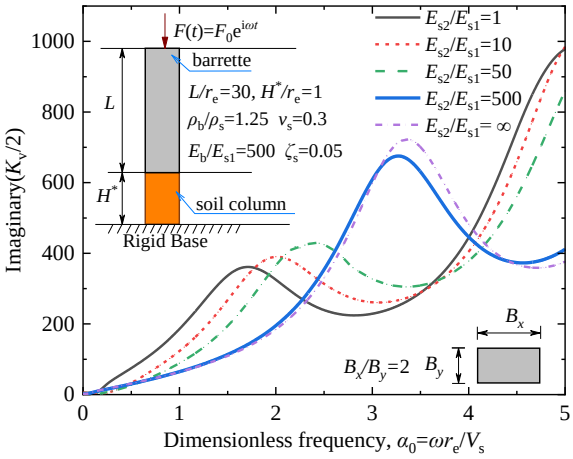


(b)

Fig. 12 Effect of module ratio of substratum to the upper soil layers on the complex barrette-head stiffness ($L/r_e$=30)

Fig. 8 that the values of real and imaginary part of barrette-head stiffness increase as the slenderness ratio of barrette increases. This is a result of the fact that the dynamic pile-head stiffness is mainly dependent on its static stiffness at the low frequencies, and the static pile-head stiffness of a floating pile increases with increase in slenderness ratio (Poulos 1989, Zheng *et al.* 2017b).

### *5.3 Influence of soil column depth*

Figs. 9 and 10 show the influences of the soil column depth $H^*$ on the complex barrette-head stiffness for two slenderness ratio $L/r_e$=10 and $L/r_e$ =30. We can observe that resonance frequencies decrease with the increase of soil column depth, and the oscillation amplitudes of the complex barrette-head stiffness decrease with increasing depth of soil column, obviously seen in Fig. 10. Moreover, the real and imaginary components of complex barrette-head stiffness are insensitive to the depth of soil column when $H^*/r_e$ exceeds 5. That means that there exists a "critical depth" of the soil column, and beyond it the complex barrette-head stiffness do not exhibit significant variations.

Meanwhile, it can be found by comparing the Fig. 9 and Fig. 10 that the variation amplitudes of the real and imaginary components decrease as the slenderness ratio increases. This results from the fact that the effect of substratum soil layer becomes weaker as the slenderness ratio of barrette increases.

Fig. 11 presents the influence of soil column depth in the complex resistance stiffness with slenderness ratio $L/r_e$=10. Note that the depth of soil column underlying the barrette base has a prominent influence not only on the oscillation amplitudes of the complex resistance stiffness, but on the resonance frequencies, both of which decrease with the increasing $H^*$. Results depicted in Fig. 11 reveal also that when the frequencies exceed the resonance frequencies, the resistance stiffness is independent to the thickness of soil column. This behavior can be understood, given that the wave generated from the vertical vibration of pile is inclined to propagate horizontally regardless of the vertical dimension (Anoyatis and Mylonakis 2012, Mylonakis 2001).

### *5.4 Influence of soil layers module ratio*

Fig. 12 presents the effects of module ratio of substratum to the upper soil layers on the complex barrette-

head stiffness in two layers, while maintaining the depth of soil column as a constant ($H^*/r_e$=1). It can be found that the oscillation phase of the complex barrette-head stiffness is sensitive the module ratio of substratum to the upper soil layers $E_{s2}/E_{s1}$, and the oscillation patterns is practically opposite for the cases $E_{s2}/E_{s1}$=1 and $E_{s2}/E_{s1}$=∞. This is mainly due to the phase difference between the natural frequencies of the friction barrette and end bearing barrette. In addition, the resonance frequencies increase with the increase of module ratio of substratum to the upper soil layers, and the oscillation amplitudes also increase as the relative modulus increase. This indicates that even the bearing capacity of ending barrette is larger than that of the friction barrette, the seismic effect of ending barrette is not as good as the friction barrette.

## 6. Conclusions

A semi-analytical method is proposed for investigating the dynamic response of axially loaded rectangular barrette. The method overcomes the complexities and difficulties in analyzing the non-axisymmetric mechanical behavior of rectangular barrette, and well captures influence of the rectangular section and finite soil layers underneath the barrette toe on the vertically dynamic response. And through using the modified Vlasov foundation model and employing Hamilton's variational principle, the governing equations for the unknown displacement and separable functions are directly derived. The solution is obtained by virtue of the iterative algorithm. Numerical examples are carried out to study the effects on the complex barrette-head stiffness and resistance stiffness. The following conclusions can be summarized:

(1) The dynamic equilibrium equation of barrette motion is composed of the axial resistances, shaft resistance and the axial inertia forces of the barrette. The shaft resistance and the resistance stiffness of barrette with rectangular cross section were obtained analytically as the sum of three parts. The first part can be considered as the Winkler spring due to the soil resistance against shearing, the second represents resistance of the soil against vertical compression, and the third accounts for the contribution of the participating soil mass.

(2) The aspect ratio of rectangular cross sections affects the complex barrette-head stiffness, and the real and imaginary part of the complex stiffness increase as the aspect ratio increases. The real and imaginary part of the complex stiffness increase with the increasing slenderness ratio of barrette.

(3) The oscillation amplitudes and resonance frequencies of the complex barrette-head stiffness decrease as the depth of soil column increase, but there exists a critical depth of the soil column, and beyond it the complex barrette-head stiffness do not exhibit significant variations. The oscillation phase and oscillation amplitudes of the complex barrette-head stiffness increase with the increasing module ratio of the substratum to upper soil layers.

## Acknowledgments

The study presented herein is supported by the National Natural Science Foundation of China (Nos. 51808112; 51678145), the Natural Science Foundation of Jiangsu Province (BK20180155), and the Six Talent Peaks Project in Jiangsu Province (No. XNY-047). The authors are grateful for their support.

## References

Ai, Z.Y. and Li, Z.X. (2015), "Dynamic analysis of a laterally loaded pile in a transversely isotropic multilayered half-space", *Eng. Anal. Bound Elem.*, **54**, 68-75. https://doi.org/10.1016/j.enganabound.2015.01.008.

Anoyatis, G. and Mylonakis, G. (2012), "Dynamic Winkler modulus for axially loaded piles", *Geotechnique*, **62**(6), 521-536. https://doi.org/10.1680/geot.11.P.052.

Basu, D., Prezzi, M., Salgado, R. and Chakraborty, T. (2008), "Settlement analysis of piles with rectangular cross sections in multi-layered soils", *Comput. Geotech.*, **35**(4), 563-575. https://doi.org/10.1016/j.compgeo.2007.09.001.

Cai, Y., Liu, Z., Li, T., Yu, J. and Wang, N. (2020), "Vertical dynamic response of a pile embedded in radially inhomogeneous soil based on fictitious soil pile model", *Soil Dyn. Earthq. Eng.*, **132**, 106038. https://doi.org/10.1016/j.soildyn.2020.106038.

Cui, C.Y., Zhang, S.P., Yang, G. and Li, X.F. (2016), "Vertical vibration of a floating pile in a saturated viscoelastic soil layer overlaying bedrock", *J. Cent. South U.*, **23**(1), 220-232. https://doi.org/10.1007/s11771-016-3065-5.

Cui, C.Y., Meng, K., Wu, Y.J., Chapman, D. and Liang, Z.M. (2018a), "Dynamic response of pipe pile embedded in layered visco-elastic media with radial inhomogeneity under vertical excitation", *Geomech. Eng.*, **16**(6), 609-618. https://doi.org/10.12989/gae.2018.16.6.609.

Cui, C., Zhang, S., Chapman, D. and Meng, K. (2018b), "Dynamic impedance of a floating pile embedded in poro-visco-elastic soils subjected to vertical harmonic loads", *Geomech. Eng.*, **15**(2), 793-803. https://doi.org/10.12989/gae.2018.15.2.793.

Das, Y.C. and Sargand, S.M. (1999), "Forced vibrations of laterally loaded piles", *Int. J. Solids Struct.*, **36**(33), 4975-4989. https://doi.org/10.1016/S0020-7683(98)00231-5.

Dym, C.L. and Shames, I.H. (1973), *Solid Mechanics: A Variational Approach*, McGraw-Hill, New York, U.S.A.

El Gendy, M., Ibrahim, H. and El Arabi, I. (2018), "Modeling single barrettes as elastic support by CCT", *Malaysian J. Civ. Eng.*, **30**(2),296-312. https://doi.org/10.11113/mjce.v30n2.481.

El Gendy, M., Ibrahim, H. and El Arabi, I. (2019), "Composed coefficient technique for barrette group", *Malaysian J. Civ. Eng.*, **31**(1), 23-33. https://doi.org/10.11113/mjce.v31n1.510.

El Wakil, A.Z. and Nazir, A.K. (2013), "Behavior of laterally loaded small scale barrettes in sand", *Ain Shams Eng. J.*, **4**(3), 343-350. http://doi.org/10.1016/j.asej.2012.10.011.

Fellenius, B.H., Altaee, A., Kulesza, R. and Hayes, J. (1999), "O-cell testing and FE analysis of 28-m-deep barrette in Manila, Philippines", *J. Geotech. Geoenviron. Eng.*, **125**(7), 566-575. https://doi.org/10.1061/(ASCE)1090-0241(1999)125:7(566).

Gan, S., Zheng, C., Kouretzis, G. and Ding, X. (2020), "Vertical vibration of piles in viscoelastic non-uniform soil overlying a rigid base", *Acta Geotech.*, **15**, 1321-1330. https://doi.org/10.1007/s11440-019-00833-7.

Guo, W.D. and Lee, F.H. (2001), "Load transfer approach for laterally loaded piles", *Int. J. Numer. Anal. Meth. Geomech.*, **25**(11), 1101-1129. https://doi.org/10.1002/nag.169.

Gupta, B.K. and Basu, D. (2016a), "Analysis of laterally loaded rigid monopiles and poles in multilayered linearly varying soil", *Comput. Geotech.*, **72**, 114-125.

https://doi.org/10.1016/j.compgeo.2015.11.008.
Gupta, B.K. and Basu, D. (2016b), "Response of laterally loaded rigid monopiles and poles in multi-layered elastic soil", *Can. Geotech. J.*, **53**(8), 1281-1292. https://doi.org/10.1139/cgj-2015-0520.
Gupta, B.K. and Basu, D. (2017), "Analysis of laterally loaded short and long piles in multilayered heterogeneous elastic soil", *Soils Found.*, **57**(1), 92-110. https://doi.org/10.1016/j.sandf.2017.01.007.
Gupta, B.K. and Basu, D. (2018), "Applicability of Timoshenko, Euler–Bernoulli and rigid beam theories in analysis of laterally loaded monopiles and piles", *Géotechnique*, **68**(9), 772-785. https://doi.org/10.1680/jgeot.16.P.244.
Gupta, B.K. and Basu, D. (2018), "Dynamic analysis of axially loaded end-bearing pile in a homogeneous viscoelastic soil", *Soil Dyn. Earth. Eng.*, **111**, 31-40. https://doi.org/10.1016/j.soildyn.2018.04.019.
Hirai, H. (2014), "Settlement analysis of rectangular piles in nonhomogeneous soil using a Winkler model approach", *Int. J. Numer. Anal. Meth. Geomech.*, **38**(12), 1298-1320. https://doi.org/10.1002/nag.227.
Kim, Y.S. and Choi, J.I. (2017), "Nonlinear numerical analyses of a pile-soil system under sinusoidal bedrock loadings verifying centrifuge model test results", *Geomech. Eng.*, **12**(2), 239-255. https://doi.org/10.12989/gae.2017.12.2.239.
Kramer, S.L. (1996), *Geotechnical Earthquake Engineering*, Prentice-Hall, Upper Saddle River, New Jersey, U.S.A.
Kuhlemeyer, R.L. (1979), "Static and dynamic laterally loaded floating piles", *J. Geotech. Eng.*, **105**, 289-304.
Lee, K. and Xiao, Z. (1999), "A new analytical model for settlement analysis of a single pile in multi-layered soil", *Soils Found.*, **39**(5), 131-143. https://doi.org/10.3208/sandf.39.5_131.
Lei, G., Hong, X. and Shi, J. (2005), "Stata-of-the-art review on barrette", *China Civ. Eng. J.*, **38**(4), 103-110 (in Chinese). https://doi.org/10.3321/j.issn:1000-131X.2005.04.017.
Lei, G.H., Hong, X. and Shi, J.Y. (2007a), "Approximate three-dimensional analysis of rectangular barrette-soil-cap interaction", *Can. Geotech. J.*, **44**(7),781-796. https://doi.org/10.1139/t07-017.
Lei, G.H. and Ng, C.W. (2007b), "Rectangular barrettes and circular bored piles in saprolites", *Proc. Inst. Civ. Eng. Geotech. Eng.*, **160**(4), 237-242. https://doi.org/10.1680/geng.2007.160.4.237.
Liu, W. and Novak, M. (1994), "Dynamic response of single piles embedded in transversely isotropic layered media", *Earthq. Eng. Struct. Dyn.*, **23**(11), 1239-1257. https://doi.org/10.1002/eqe.4290231106.
Maeso, O., Aznárez, J.J. and García, F. (2005), "Dynamic impedances of piles and groups of piles in saturated soils", *Comput. Struct.*, **83**(10-11), 769-782. https://doi.org/10.1016/j.compstruc.2004.10.015.
Mamoon, S.M., Kaynia, A.M. and Banerjee, P.K. (1990), "Frequency domain dynamic analysis of piles and pile groups", *J. Eng. Mech.*, **116**(10), 2237-2257. https://doi.org/10.1061/(ASCE)0733-9399(1990)116:10(2237).
Michaelides, O., Gazetas, G., Bouckovalas, G. and Chrysikou, E. (1998), "Approximate non-linear dynamic axial response of piles", *Geotechnique*, **48**(1), 33-53. https://doi.org/10.1680/geot.1998.48.1.33.
Millan, M.A. and Dominguez, J. (2009), "Simplified BEM/FEM model for dynamic analysis of structures on piles and pile groups in viscoelastic and poroelastic soils", *Eng. Anal. Bound Elem.*, **33**(1), 25-34. https://doi.org/10.1016/j.enganabound.2008.04.003.
Mylonakis, G. (2001), "Elastodynamic model for large-diameter end-bearing shafts", *Soils Found.*, **41**(3), 31-44. https://doi.org/10.3208/sandf.41.3_31.
Mylonakis, G. and Gazetas, G. (1998), "Settlement and additional internal forces of grouped piles in layered soil", *Geotechnique*, **48**(1), 55-72. https://doi.org/10.1680/geot.1998.48.1.55.
Ng, C.W. and Lei, G.H. (2003), "Performance of long rectangular barrettes in granitic saprolites", *J. Geotech. Geoenviron. Eng.*, **129**(8), 685-696. https://doi.org/10.1061/(ASCE)1090-0241(2003)129:8(685).
Ng, C.W., Rigby, D.B., Ng, S.W. and Lei, G.H. (2000), "Field studies of well-instrumented barrette in Hong Kong", *J. Geotech. Geoenviron. Eng.*, **126**(1), 60-73. https://doi.org/10.1061/(ASCE)1090-0241(2000)126:1(60).
Nogami, T. and Konagai, K. (1987), "Dynamic response of vertically loaded nonlinear pile foundations", *J. Geotech. Eng.*, **113**(2), 147-160. https://doi.org/10.1061/(ASCE)0733-9410(1987)113:2(147).
Padron, L.A., Aznarez, J.J. and Maeso, O. (2007), "BEM-FEM coupling model for the dynamic analysis of piles and pile groups", *Eng. Anal. Bound Elem.*, **31**(6), 473-484. https://doi.org/10.1016/j.enganabound.2006.11.001.
Poulos, H.G. (1989), "Pile behaviour—theory and application", *Geotechnique*, **39**(3), 365-415. https://doi.org/10.1680/geot.1989.39.3.365.
Randolph, M.F. (1981), "The response of flexible piles to lateral loading", *Geotechnique*, **31**(2), 247-259. https://doi.org/10.1680/geot.1981.31.2.247.
Seo, H., Basu, D., Prezzi, M. and Salgado, R. (2009), "Load-settlement response of rectangular and circular piles in multilayered soil", *J. Geotech. Geoenviron. Eng.*, **135**(3), 420-430. https://doi.org/10.1061/(ASCE)1090-0241(2009)135:3(420).
Sun, K. (1994a), "Laterally loaded piles in elastic media", *J. Geotech. Eng.*, **120**(8), 1324-1344. https://doi.org/10.1061/(ASCE)0733-9410(1994)120:8(1324).
Sun, K. (1994b), "A numerical method for laterally loaded piles", *Comput. Geotech.*, **16**(4), 263-289. https://doi.org/10.1016/0266-352X(94)90011-6.
Tehrani, F.S., Salgado, R. and Prezzi, M. (2016), "Analysis of axial loading of pile groups in multilayered elastic soil", *Int. J. Geomech.*, **16**(2), 04015063. https://doi.org/10.1061/(ASCE)GM.1943-5622.0000540.
Ukritchon, B. and Keawsawasvong, S. (2018), "Undrained lateral capacity of rectangular piles under a general loading direction and full flow mechanism", *KSCE J. Civ. Eng.*, **22**(7), 2256-2265. https://doi.org/10.1007/s12205-017-0062-7.
Vallabhan, C.G. and Das, Y.C. (1988), "Parametric study of beams on elastic foundations", *J. Eng. Mech.*, **114**(12), 2072-2082. https://doi.org/10.1061/(ASCE)0733-9399(1988)114:12(2072)
Vallabhan, C.G. and Das, Y.C. (1991a), "Modified Vlasov model for beams on elastic foundations", *J. Geotech. Eng.*, **117**(6), 956-966. https://doi.org/10.1061/(ASCE)0733-9410(1991)117:6(956).
Vallabhan, C.G. and Das, Y.C. (1991b), "Analysis of circular tank foundations", *J. Eng. Mech.*, **117**(4), 789-797. https://doi.org/10.1061/(ASCE)0733-9399(1991)117:4(789).
Vallabhan, C.G. and Mustafa, G. (1996), "A new model for the analysis of settlement of drilled piers", *Int. J. Numer. Anal. Meth. Geomech.*, **20**(2), 143-152. https://doi.org/10.1002/(SICI)10969853(199602)20:2<143::AID-NAG812>3.0.CO;2-U.
Veletsos, A.S. and Dotson, K.W. (1986), "Impedances of soil layer with disturbed boundary zone", *J. Geotech. Eng.*, **112**(3), 363-368. https://doi.org/10.1061/(ASCE)0733-9410(1986)112:3(363).
Wang, K., Wu, W., Zhang, Z. and Leo, C. J. (2010), "Vertical dynamic response of an inhomogeneous viscoelastic pile", *Comput. Geotech.*, **37**(4), 536-544. https://doi.org/10.1016/j.compgeo.2010.03.001.

Wu, W.B., Liu, H., El Naggar, M.H., Mei, G.X. and Jiang, G.S. (2016), "Torsional dynamic response of a pile embedded in layered soil based on the fctitious soil pile model", *Comput*. *Geotech*., **80**, 190-198. https://doi.org/10.1016/j.compgeo.2016.06.013.

Wu, W.B., Liu, H., Yang, X.Y., Jiang, G.S., El Naggar, M.H., Mei, G.X. and Liang, R.Z. (2020), "New method to calculate apparent phase velocity of open-ended pipe pile", *Can*. *Geotech*. *J*., **57**(1), 127-138. https://doi.org/10.1139/cgj-2018-0816.

Wu, W.B., Wang, K.H., Zhang, Z.Q. and Leo, C.J. (2013), "Soil-pile interaction in the pile vertical vibration considering true three-dimensional wave effect of soil", *Int*. *J*. *Numer*. *Anal*. *Meth*. *Geomech*., **37**(17), 2860-2876. https://doi.org/10.1002/nag.2164.

Yang, D.Y. and Wang, K.H. (2010), "Vertical vibration of pile based on fctitious soil-pile model in inhomogeneous soil", *J*. *Zhejiang Univ*., **44**(10), 2021-2028 (in Chinese). https://doi.org/10.3785/j.issn.1008-973X.2010.10.030.

Zhang, L.M. (2003), "Behavior of laterally loaded large-section barrettes", *J*. *Geotech*. *Geoenviron*. *Eng*., **129**(7), 639-648. https://doi.org/10.1061/(ASCE)1090-0241(2003)129:7(639).

Zheng, C., Ding, X., Li, P. and Fu, Q. (2015), "Vertical impedance of an end-bearing pile in viscoelastic soil", *Int*. *J*. *Numer*. *Anal*. *Meth*. *Geomech*., **39**(6), 676-684. https://doi.org/10.1002/nag.2324.

Zheng, C., Liu, H., Ding, X. and Kouretzis, G. (2017a), "Resistance of inner soil to the vertical vibration of pipe piles", *Soil Dyn*. *Earthq*. *Eng*., **94**, 83-87. https://doi.org/10.1016/j.soildyn.2017.01.002.

Zheng, C., Gan, S., Ding, X. and Luan, L. (2017b), "Dynamic response of a pile embedded in elastic half space subjected to harmonic vertical loading", *Acta Mech*. *Solida Sin*., **30**(6), 668-673. https://doi.org/10.1016/j.camss.2017.09.006.

*CC*

## Appendix A. The solution fo 2*n* unknown constants

We express the algebraic equations in matrix form as follows

$$\mathbf{MC} = \mathbf{B} \tag{A-1}$$

where

$$\mathbf{C}^T = \{c_{11} \quad c_{21} \quad c_{12} \quad c_{22} \quad \mathrm{L} \quad c_{1i} \quad c_{2i} \quad \mathrm{L} \quad c_{1m} \quad c_{2m} \quad \mathrm{L} \quad c_{1n} \quad c_{2n}\} \tag{A-2}$$

$$\mathbf{B}^T = \{-F_0 \quad 0 \quad 0 \quad 0 \quad \mathrm{L} \quad 0 \quad 0 \quad \mathrm{L} \quad 0 \quad 0 \quad \mathrm{L} \quad 0 \quad 0\} \tag{A-3}$$

$$\mathbf{M} = \begin{bmatrix}
\bar{b}_{11} & \bar{b}_{21} & 0 & 0 & \mathrm{L} & 0 & 0 & 0 & 0 & \mathrm{L} & 0 & 0 & 0 & 0 \\
a_{11} & a_{21} & -\bar{a}_{12} & -\bar{a}_{22} & \mathrm{L} & 0 & 0 & 0 & 0 & \mathrm{L} & 0 & 0 & 0 & 0 \\
b_{11} & b_{21} & -\bar{b}_{12} & -\bar{b}_{22} & \mathrm{L} & 0 & 0 & 0 & 0 & \mathrm{L} & 0 & 0 & 0 & 0 \\
\mathrm{M} & \mathrm{M} & \mathrm{M} & \mathrm{M} & \mathrm{O} & \mathrm{M} & \mathrm{M} & \mathrm{M} & \mathrm{M} & \mathrm{L} & 0 & 0 & 0 & 0 \\
0 & 0 & 0 & 0 & 0 & a_{1m} & a_{2m} & -\bar{a}_{1,m+1} & -\bar{a}_{2,m+1} & \mathrm{L} & 0 & 0 & 0 & 0 \\
0 & 0 & 0 & 0 & 0 & b_{1m} & b_{2m} & -\bar{b}_{1,m+1} & -\bar{b}_{2,m+1} & \mathrm{L} & 0 & 0 & 0 & 0 \\
\mathrm{M} & \mathrm{M} & \mathrm{M} & \mathrm{M} & \mathrm{M} & \mathrm{M} & \mathrm{M} & \mathrm{M} & \mathrm{M} & \mathrm{O} & 0 & 0 & 0 & 0 \\
0 & 0 & 0 & 0 & 0 & 0 & 0 & 0 & 0 & 0 & a_{1n-1} & a_{2n-1} & -\bar{a}_{1n} & -\bar{a}_{2n} \\
0 & 0 & 0 & 0 & 0 & 0 & 0 & 0 & 0 & 0 & b_{1n-1} & b_{2n-1} & -\bar{b}_{1n} & -\bar{b}_{2n} \\
0 & 0 & 0 & 0 & 0 & 0 & 0 & 0 & 0 & 0 & 0 & 0 & a_{1n} & a_{2n}
\end{bmatrix} \tag{A-4}$$

where

$$a_{1i} = e^{r_{bi}H_i}, \quad a_{2i} = e^{-r_{bi}H_i} \quad b_{1i} = q_{bi}r_{bi}e^{r_{bi}H_i}, \quad b_{2i} = -q_{bi}r_{bi}e^{-r_{bi}H_i}, \quad q_{bi} = E_{\mathrm{b}}A + t_i \qquad i = 1,2,\ldots,m$$

$$a_{1i} = e^{r_{si}H_i}, \quad a_{2i} = e^{-r_{si}H_i}, \quad q_{si} = E_{\mathrm{s}}A + t_i \quad b_{1i} = q_{si}r_{si}e^{r_{si}H_i}, \quad b_{1i} = -q_{si}r_{si}e^{-r_{si}H_i}, \qquad i = m+1, m+2, \ldots, n$$

$$\bar{a}_{1i} = e^{r_{bi}H_{i-1}}, \quad \bar{a}_{2i} = e^{-r_{bi}H_{i-1}}, \quad \bar{b}_{1i} = q_{bi}r_{bi}e^{r_{bi}H_{i-1}}, \quad \bar{b}_{2i} = -q_{bi}r_{bi}e^{-r_{bi}H_{i-1}} \qquad i = 1,2,\ldots,m$$

$$\bar{a}_{1i} = e^{r_{si}H_{i-1}}, \quad \bar{a}_{2i} = e^{-r_{si}H_{i-1}}, \quad \bar{b}_{1i} = q_{si}r_{si}e^{r_{si}H_{i-1}}, \quad \bar{b}_{2i} = -q_{si}r_{si}e^{-r_{si}H_{i-1}} \qquad i = m+1, m+2, \ldots, n$$